Carbon dioxide removal could result in the use of lower-grade iron ore in a decarbonized net-negative emission steel industry

Renforth, P.[1*], Campbell, J.[1], Foteinis, S. [1], Cosgun, E.[1], Young, J. [1], Strunge, T.[1], Riley, A.L. [2], Mayes, W. M.[2], van der Spek, M.W.[1]

1. Research Centre for Carbon Solutions, Heriot-Watt University, Edinburgh, EH14 4AS, UK
2. School of Environmental Sciences, University of Hull, Cottingham Road, Hull HU6 7RX, UK

*p.renforth@hw.ac.uk

Reducing the emissions from steel production is essential in meeting climate targets while maintaining economic prosperity. Here we show that applying deep emissions mitigation to the steel industry together with the reaction of by-product slag with atmospheric carbon dioxide (CO_2) could result in a carbon negative industry on the order of up to a $GtCO_2$ yr^{-1} by mid-century. We used a bespoke technoeconomic assessment model that simulates a base-case scenarios in which steel is produced using a blast furnace and basic oxygen furnace. This system was augmented with a range of climate change intervention technologies including biomass based reducant, directly reduced iron, carbon capture and storage, and slag carbonation. Surprisingly, strong incentivisation ($200 – 500 tCO_2^{-1}) for emissions reduction and CO_2 removal from the atmosphere may create conditions under which lower grade ores are commercially viable and also achieve deep emissions mitigation. The additional costs for emissions reduction could be wholly offset by value generated through carbon removal from biomass energy carbon capture and storage together with slag carbonation.

1.0 Introduction

The commitment of 188 countries and the European Union to limit climate change to less than 2°C by ratifying, or acceding to, the Paris Agreement (Paris Agreement, 2015) implies that the cumulative emission of greenhouse gasses into the atmosphere should not exceed more than 1000 billion tonnes (Gt) CO_2-eq over preindustrial levels (Allen et al., 2009). Therefore, in addition to reductions in current emission (e.g., via energy system transformation and behavioural change), processes that remove CO_2 from the atmosphere, known as 'carbon dioxide removal' (CDR) will be needed to offset residual emissions for net-zero targets and pathways that overshoot and recover (Masson-Delmotte et al., 2022). A range of approaches have been proposed for removing CO_2 from the atmosphere the most prominent of which use biomass in electricity generation coupled with carbon capture and storage (CCS), or the use of sorbents to directly scrub CO_2 from the atmosphere for geological storage(Committee on Developing a Research Agenda for Carbon Dioxide Removal and Reliable Sequestration et al., 2019).

The steel industry emits approximately 4 $GtCO_2$ per year globally while creating 1.9 Gt of steel (4-5% of global CO_2 emissions)(World Steel Association, 2023). Contemporary methods of steel production rely on the creation of CO_2 during the reduction of iron oxides in the ore (e.g., Equation 1), the calcination of carbonates to flux with impurities (clay or silica) within the ore (e.g., Equation 2), and from the fossil fuel-based energy to heat the furnace to >1,500°C (e.g., Equation 3). These intrinsic CO_2 creating processes, together with the wider indirect greenhouse emissions from the industry and its supply chain, suggest that steel production may be difficult to decarbonise.

$$Fe_2O_3 + 1.5C \rightarrow 2Fe + 1.5CO_2 \qquad \text{Equation 1}$$

$$3CaCO_3 + Al_2Si_2O_5(OH)_4 \xrightarrow{\square} Ca_2Al_2SiO_7 + CaSiO_3 + 2H_2O + 3CO_2$$ Equation 2

$$C + O_2 \xrightarrow{\square} CO_2$$ Equation 3

Strategies for emissions reduction in the steel industry consider alternative low carbon reductants and energy vectors (e.g., biomass based, or hydrogen produced from low carbon electricity (Mousa et al., 2016; Otto et al., 2017; Ren et al., 2021)), energy demand reduction through greater efficiencies, increased use of scrap metal as a feedstock, decarbonising the supply chain, and CCS (Fan and Friedmann, 2021; Tanzer et al., 2020). Production of directly reduced iron (DRI) using natural gas or hydrogen is another promising technology for emissions reduction that is being developed (Fan and Friedmann, 2021). By developing and deploying these technologies, CO_2 emissions from the steel sector may reduce to <2 $GtCO_2$ yr^{-1} by 2050, while production of steel increases to >2Gt yr^{-1} (International Energy Agency, 2020) (Supplementary Text 1).

No prominent roadmaps for steel decarbonisation include the reaction of by-product slag with CO_2. While the chemical composition, mineralogy, and physical property of slag varies depending on raw materials, production and disposal methods, its reaction with CO_2 can be generally described as a reaction with a metal oxide/hydroxide (Equation 4) or a silicate mineral (Equation 5).

$$Ca(OH)_2 + CO_2 \xrightarrow{\square} CaCO_3 + H_2O$$ Equation 4

$$CaSiO_3 + CO_2 \xrightarrow{\square} CaCO_3 + SiO_2$$ Equation 5

Slag from iron and steel production may be able to capture 370-420 $kgCO_2$ t^{-1} based on its chemical composition (Renforth, 2019), which is equivalent to ~100-150 $kgCO_2$ $t(steel)^{-1}$ or 5-8% of current emissions. Slag carbonation could become increasingly important in pathways for low emission steel. Uptake of atmospheric CO_2 at legacy deposits of slag has been reported (Mayes et al., 2018; Renforth et al., 2009), but carbon mass balance of this material suggests that only a small proportion of the carbon capture potential has been achieved (Pullin et al., 2019). Engineered solutions for slag carbonation have been proposed under a variety of reactor conditions (Bonenfant et al., 2008; Huijgen et al., 2005; Huijgen and Comans, 2006) with estimated costs ~$115 tCO_2^{-1} (Huijgen et al., 2007). Other approaches include reaction of alkaline materials such as slag with CO_2 in air in humidified tiered greenhouses(Myers and Nakagaki, 2020), or agitated aqueous ponds (Dubey et al., 2002). Stolaroff et al.(2005) proposed a low-cost ($10 tCO_2^{-1}) method whereby large heaps of slag are gravity-leached using water. The resulting calcium-rich leachate was sprayed into the air to capture CO_2, then recirculated through the slag pile, causing the eventual build-up of stable $CaCO_3$ (Supplementary Text 2). Spreading of slag on agricultural or forest land for enhanced weathering have also been investigated (Zhang et al., 2023), but potential release of ecotoxic metal(loid)s (particularly As, Cr, V), hyper alkaline buffering of porewaters, or rapid carbonate precipitation toxicological considerations would require careful monitoring (Wendling et al., 2013). Studies do however, suggest that leaching risks are relatively low for iron and steel by-products in a range of weathering settings (Hobson et al., 2018; Riley et al., 2023). To increase carbonation kinetics atmospheric CO_2 can be supplied to the reaction via direct air capture (DAC), which is the engineered direct removal of CO_2 from the air (Küng et al., 2023). Current DAC technologies are designed to produce pure CO_2 for geologic sequestration. However, it may be possible to design a DAC process optimised to supply lower purity CO_2 at a reduced energy penalty and cost for slag heap carbonation (Supplementary Text 3).

Presently, steel is the valued commodity produced by the steel industry (~ >$800 t^{-1}). However, nearly all slag from blast furnaces goes into beneficial afteruses, with the majority granulated for use in cement and concrete production (up to 89% in some jurisdictions (Strunk, 2020)). The demand for slag cement has doubled in the last decade and looks set to continue given the carbon benefits granulated blast furnace (BF) slag has in substituting virgin limestone calcination in cement production (Guo et al., 2018). Other civil engineering applications (e.g. aggregate or road base) and niche applications (e.g. as a fertiliser) represent other key downstream uses of BF slag. Basic oxygen furnace (BOF) slag also has a range of potential revenue-generating afteruses, but reuse rates are typically lower than BF slag with recycling rates varying from 100% down to ~20% (Nunes and Borges, 2021; Strunk, 2020). Key afteruses for this slag are in civil engineering applications (e.g. roadbase, fill material, land reclamation) which may require a period of 'weathering' (typically 6 months)(Hobson et al., 2018). By-product slag can return values up to ~$150 t^{-1} when used as a cement, but the majority is low value <$10 t^{-1} (e.g., used as secondary aggregate) and is often stockpiled at steelworks (Deutz et al., 2017). (Supplementary Text 2)

Here we explore the combined impact of emissions reduction and CO_2 removal on the steel industry, through the creation of a technoeconomic model of a steelworks. The base case scenario simulates a BF-BOF steelworks with additional scenarios simulating a range of decarbonisation interventions (biomass substitution, decarbonised power supply, directly reduced iron using hydrogen produced on-site, and CCS through calcium looping) and the reaction of atmospheric CO_2 with slag. We also explore the use of lower-grade ores, which would increase the production of slag (and thus the removal of atmospheric CO_2). The reaction of slag with atmospheric CO_2 may provide an opportunity for a decarbonised steel industry to achieve net negative emissions.

2.0 Material and Methods

A bottom up technoeconomic model that simulates mass and energy balance across an idealised integrated steelworks was specified in Python (v3.9.12, in Spyder IDE v5.1.5), which allowed for the rapid calculation of mass and energy balance across the range of components of the steelworks, and to assess the uncertainty in the assumptions. Here, we explore changes to the foreground technology by implementing a range of climate change interventions, while maintaining constant assumptions of background technoeconomic context. A prognostic technoeconomic assessment was undertaken by exploring projections of background assumptions with a gradual foreground technology transition. The model is fully described in Supplementary Text 5 to 11, and Figure 1, but we have included a summary here. The model code is freely available from https://doi.org/10.17861/e9765431-e8cc-4834-8cde-e859347c42be .

The base-case system simulates the reduction of 4.1 Mt a^{-1} of iron ore using a blast furnace (BF) and basic oxygen furnace (BOF) (the mass flow was selected for consistency with the primary source of capital cost data (Hooey et al., 2013)), a technology which currently facilitates approximately 70% of global steel production, and may continue to contribute up to 35-50% through to 2050 even under ambitious mitigation scenarios (International Energy Agency, 2020). An electric arc furnace (EAF) was also implemented in the model to simulate scrap metal recycling. The flow of scrap metal to the EAF was controlled such that the secondary production of steel was approximately 22% of the total steel produced (consistent with contemporary scrap utilisation globally (Wang et al., 2021)). The mass flow of material thorough the base-case is presented in Supplementary Table 2.

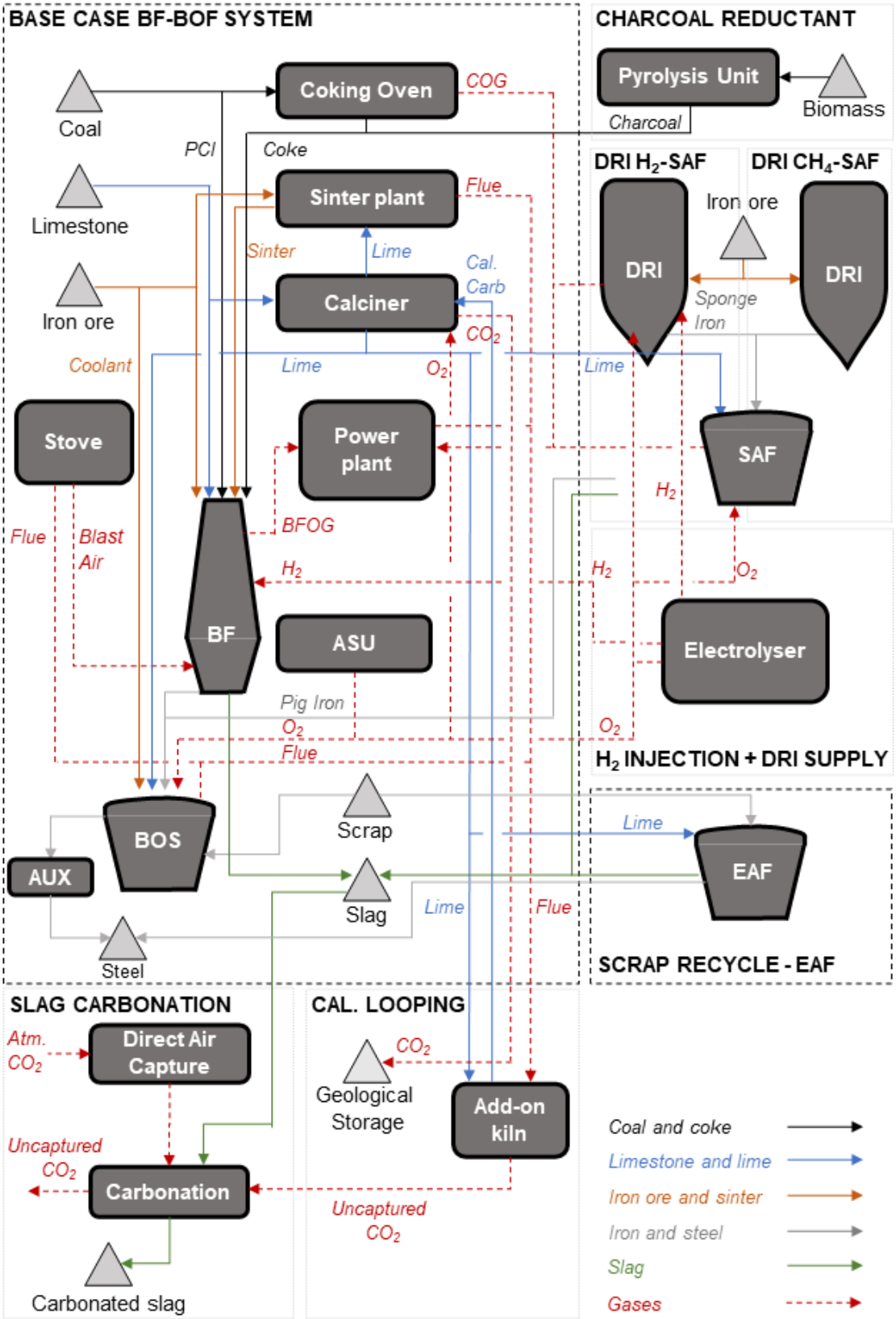

Figure 1: A summary schematic of the mass flows in the integrated steelworks model. The base case BF-BOF is highlighted, as are the range of climate change interventions. The model is constructed to be indicative of the steel industry, rather than a single production site.

2.1 Mass and energy balance of blast furnace.

The model assumes that 50% of the iron ore of a predefined grade (base case 65% Fe) is added to the blast furnace as lump ore and the remaining material is sintered. Fe in the ore is assumed to be distributed between 85% magnetite (Fe_2O_3) and 15% wüstite (FeO), which constitute 91% of the total mass of the ore (Bhattacharya and Muthusamy, 2017; Clout and Manuel, 2015; Kobelev et al., 2015). For simplicity, the remaining mass is assumed to be 2% moisture, 3% carbon, 2.4% silica (SiO_2), and 1.6% kaolinite ($Al_2Si_2O_6$), which is consistent with typical composition of iron ore (Bhattacharya and Muthusamy, 2017; Clout and Manuel, 2015; Kobelev et al., 2015), although excludes other base cations (Mg, Na, K) and phosphorus. For modelling experiments that decrease the ore grade, the moisture content and carbon content remain the same as above, and the contribution of silica and kaolinite were increased to compensate, and the ratio between silica and kaolinite was maintained constant. The temperature of the furnace was controlled by the chemical composition of the charge (Kobelev et al., 2015) (see Supplementary Text 5).

The blast furnace was charged with iron ore, coke, sinter, and limestone, the chemical composition of which is provided in Supplementary Table 3. The amount of limestone added to the furnace was tuned to maintain a molar ratio of calcium to silicon in the slag of 1.1 (Peacey and Davenport, 2016). The amount of reductant added to the furnace was tuned to meet the energy demand calculated through the enthalpies between the reactants and products (Supplementary Text 10), and the model assumes that 70% of this was derived from the top charged coke and the remaining supplied from pulverised coal injection. Radiative heat loss from the furnaces on the steelworks was assumed to be 10% (Rasul et al., 2007). The operating temperature of the blast furnace was calculated by estimating the chemistry of the melt (assuming a predefined Ca/Si ratio, and no ash contribution from the coke of coal injection, Supplementary Text 5).

The composition of hot metal produced in the furnace is given in Supplementary Table 3. Slag produced from a blast furnace can contain a wide range of mineral phases and amorphous silicate glass (Pullin et al., 2019). For simplicity, the composition of slag was assumed to be a mixture of a calcium silicate phase (wollastonite, $CaSiO_3$), lime (CaO), and alumina (Al_2O_3). The mineralogical composition of the slag impacts the energy balance of the furnace, however the enthalpies of slag formation for a range of minerals is provided in Supplementary Table 4, which indicates a marginal variation on wollastonite formation (10-25%), which would result in a variation of total enthalpy of the blast furnace 2-6%.

The top gas was assumed to be a mixture of carbon monoxide (CO), CO_2, water vapour, hydrogen, and nitrogen. The CO_2 to CO, and H_2O to H_2 ratios were assumed to be 0.82 and 1.0 respectively (consistent with measured data (Bhattacharya and Muthusamy, 2017)). The amount of blast gas injected into the furnace was tuned to maintain the oxygen molar balance of the furnace (equivalent to ~1200 $Nm^3\ t^{-1}$ hot metal, which is consistent with plant operation data (Bhattacharya and Muthusamy, 2017)). Heating requirements of raising the blast gas to furnace temperature was calculated through the sum of the sensible heat changes of air and accounting for a burner efficiency of 70% (4.5 MJ Nm^{-3}), electricity requirement for blowing were assumed to be 0.1 kWh Nm^{-3} (IEA, 2012).

2.2 Mass and energy balance of the sinter plant.

Iron ore of the same chemical composition of the blast furnace was added to the sinter plant along with coke and lime. Like the BF, the amounts of lime and coke were tuned to maintain sinter basicity and energy balance respectively. Gasses from the sinter plant included CO_2, water vapour, nitrogen, and excess oxygen (assumed to be 50% of the oxygen consumed in

the oxidation of carbon in the furnace). Furnace ignition energy was assumed to be fixed at 140 MJ t(sinter)$^{-1}$ and sintering electricity requirements were assumed to be 32 kWh t(sinter)$^{-1}$ (IEA, 2012).

2.3 Mass and energy balance of the basic oxygen furnace and electric arc furnace.

Hot metal from the BF, scrap metal, 'coolant' iron ore, and lime were the solid feedstock to the BOF. The hot metal to scrap ratio was maintained at 5 and the amount of lime added to the furnace was tuned to maintain a basicity of the steel slag of 3.3. The same approach was used for the EAF, although no coolant ore was used. Pure oxygen was supplied to the furnace to maintain oxygen balance, assuming that the top gas had a CO to CO_2 ratio of 1.86 (Madhavan et al., 2021) (but also contained some water vapour from moisture in the coolant). The amount of coolant added was tuned to maintain energy balance. Energy requirements for BOF ancillaries (e.g., remelting, blowing, conveyance) were assumed to be fixed at 500 MJ and 113 kWh t(steel)$^{-1}$ (IEA, 2012).

2.4 Mass and energy balance of the calciner, air separation unit, coke and steelworks ancillaries.

Lime, coke, and oxygen requirements were met through a calciner and air separation unit respectively, all with fixed energy requirements with respect to their product. All other operations on a steel works (casting, rolling, forging) were considered as a single combined 'ancillary' process. For heat and electricity requirements of these processes of see Supplementary Table 5.

2.5 Heat integration and power use.

To simulate heat integration, thermal energy demand for the steelworks (for sintering, calcination, coke production, and ancillary BF and BOF activities) is initially met through the oxidation of blast furnace and coke oven gases (assuming a utilisation efficiency of 10%) equivalent to 566 MJ t(steel)$^{-1}$ in the base case). In all the simulations, the heat requirements of the steelworks exceed what can be provided from off-gas combustion, which is supplemented with the combustion of natural gas. The model was coded to include the possibility of using a power station to generate electricity from unused chemical energy of off-gasses, but this facility was not used. Electricity demand was met in the simulations by purchasing power from a local energy grid.

2.6 Climate change intervention scenarios.

A range of climate change interventions for the steel industry have been implemented in the model (Table 1, and Supplementary Text 1). Calcium looping was selected for its possible advantages of integration with conventional steel production (Tian et al., 2018) and possibility higher capture rates compared to other technologies.

The direct reduction of iron (DRI) ore through its contact with a reducing gas (H_2 or CH_4) minimises the production of process CO_2 (Vogl et al., 2018) to produce 'sponge iron'. The model assumes a proportion of iron ore is diverted to DRI (up to 50%, Table 1), DRI using H_2 and CH_4 were simulated separately in the model, in which the relatively distribution between the two systems was 1:3 (consistent with future projections of deployment, see Supplementary Figure 2). In the former, the H_2 gas was produced from an electrolyser. The model assumes that all of the H_2 or CH_4 added to the DRI reactor is consumed and converted into H_2O, CO_2, or CO, the amount of which is tuned to maintain oxygen balance between reactants and products (66 kgH_2 t(sponge)$^{-1}$ and 250 Nm^3 CH_4 in Scenario A at

65% Fe). Cabon in the ore is assumed oxidised to CO_2 or CO with a ratio of 0.82 (consistent with a typical top gas composition (Bhattacharya and Muthusamy, 2017)). Energy is balanced within the furnace by the introduction of additional O_2 (0.45 tO_2 $t(sponge)^{-1}$ Scenario A at 65% Fe) derived either from the electrolyser or air separation unit. Given the slag limits of conventional electric arc furnace, the sponge iron produced from DRI was refined into iron using a submerged arc furnace(Friedrich et al., 2018) (although the capital costs were assumed to be the same as an electric arc furnace (Steelonthenet, 2023), which was further refined into steel using the BOF.

A pyrolizer is used in the model to convert biomass into charcoal, with a conversion of 3.3 tonnes of biomass per tonne of charcoal created (Jesus et al., 2018). While the chemical composition of charcoal can be variable, for simplicity it is assumed to be identical to coke. The evolution of non-condensable gasses (CO, CO_2 and CH_4) in pyrolysis is normalised to the amount of charcoal produced, and the relative composition is assumed. Maximum charcoal substitution for nut coke is assumed to be 30%, which is conservative given that 50-100% may be possible (Mandova et al., 2018).

The amount of scrap metal fed into the EAF was increased such that secondary steel production increased from 22% to 56%.

2.7 Emissions.

In the base case scenario, all oxidised process gases and CO_2 created during natural gas combustion are emitted to the atmosphere. In all intervention scenarios it is assumed that 5% of the process gasses are emitted as fugitive (e.g., through leaking, consistent with gas processing equipment (EPA, 1995)). The CO_2 intensity of the feedstock and energy supply chains are included within the CO_2 emission of the steelworks (see Supplementary Table 6), equivalent to considering scope 1, 2 and 3 of the emissions from the steelworks. For simplicity the emissions associated with iron ore extraction/transport (~8% of total) remain the same across the range of ore grades considered, although some work suggests a range of emissions from varying ore grades (Gan and Griffin, 2018).

2.8 Sizing and costing the slag carbonation system.

A detailed explanation of the system used for carbonating steel slag is discussed in Supplementary Text 2. Slag produced from the furnaces is assumed to be composed of wollastonite ($CaSiO_3$), lime (CaO), and alumina (Al_2O_3). Hydrated lime and wollastonite react with CO_2 through Equations 4 and 5. A bespoke technoeconomic assessment was performed for ambient carbonation of slag in a large-scale, well-mixed, batch slurry reactor, (particle diameter of 53 μm, water to solids ratio of 5). The slurry reactors were sparged with pure CO_2 supplied using a stylised DAC system. The slag carbonation facility (excluding DAC) was estimated to cost \$81 tCO_2^{-1}, which is cost effective compared to the high P/T aqueous carbonation route (\$115 tCO_2^{-1}) evaluated by Huijgen et al.(2007) yet more costly than the static heap leaching system (\$10 tCO_2^{-1}) proposed by others(Stolaroff et al., 2005).

Table 1. An overview of the climate intervention strategies used in the model

Scenarios	Carbon capture and storage (%)[a]	Directly reduced iron (%)[b]	Biomass substitution as charcoal (%)I[c]	Injection of H_2 into furnace (kgH_2 t^{-1})[d]	Slag carbonation (%)[e]
Base Case	-	-	-	-	-

Scenario A	28	25	10	-	-
Scenario A + Slag carbonation					75
Scenario B	95	50	20	25	-
Scenario B+ Slag carbonation				25	75
Maximum intervention	99		30	28	

a. Proportion of the process CO_2 process gases from the site are captured through calcium looping.
b. Proportion the iron ore diverted to DRI (1:3 ratio between H_2 and CH_4).
c. Proportion of the reductant (coke) is replaced by charcoal.
d. Per tonne of hot metal.
e. of the carbonation potential of the slag is realised.

2.9 Levelised cost of production.

We calculated the levelized cost of production (LCOP) by combining the capital and operational costs ('capex' and 'opex'). The total overnight costs (TOC) were annualised using a capital charge factor (CCF = 0.12), levelized using a levelisation factor (LF = 1.2), and normalised to a capacity factor (CF = 0.95) (Equation 6). The levelisation factor is intended to account for discounting and life expectancy of the capital equipment (equating approximately to a discount rate of 8% consistent with other carbon management technologies (van der Spek et al., 2020) and a service life of 25 years typical of a project lifetime (Hooey et al., 2013)). The expression of capital within the total costs of the system was simplified given that the primary costs of steel production are well established and publicly available. Exploring the sensitivity of capital costs with a range of macro-economic drivers, or the cost sensitivity to the time dependent implementation of climate change interventions was beyond the scope of this work.

$$LCOP = \frac{LF \cdot TOC \cdot CCF}{CF} + Opex \qquad \text{Equation 6.}$$

2.10 Sizing the processes and capital costs.

Data associated with steelworks capital items was sourced from Hooey et al.,(Hooey et al., 2013) and supplemented with additional information for DRI (assumed as to be a shaft furnace (Woods, 2007)), submerged arc furnace (assumed similar to an electric arc furnace from (Facchini et al., 2021)), electrolysers (adapted from (Wörtler et al., 2013)), calcium looping (Tian et al., 2018), pyrolysis (Salman, Chaudhary Awais, 2014), and slag carbonation (see Supplementary Table 7), and converted to 2019 values using the CEPCI. Reference cost (C_{ref}) data for a given reference size (S_{ref}) was used to calculate the cost (C_{op}) of the operational size (S_{op}) of the process with the modelled steelworks using exponent (n) scaling (Equation 7).

$$C_{op} = C_{ref} \left(\frac{S_{op}}{S_{ref}}\right)^n \qquad \text{Equation 7}$$

Given that the model explores the reduction in ore purity, the reference size of the blast furnace and the melting furnace was normalised to melt volume rather than the mass of hot metal using Equation 18 in Supplementary Text 4. Given the range of maturities of the processes in this model, contingency factors (θ, 5 – 50%) were applied to specific components, and total production costs (TPC) were calculated by summing all the cost components (Equations 8).

$$TPC = \sum C_{op} \cdot \theta \qquad \text{Equation 8}$$

Total overnight costs were calculated by assuming a contribution of engineering, procurement and construction costs (EPCC = 12%) and owners costs (OC = 5%, Equation 9),

$$TOC = TPC((EPCC\ (1 + OC)) + 1) \quad \text{Equation 9}$$

2.11 Calculating process operational costs.

A range of raw material (iron ore, limestone, coal, natural gas, water, biomass, and scrap metal) and electricity costs were incorporated into the model by multiplying the annual mass or energy consumption within the steelworks to derive annual costs (Supplementary Table 8). The cost of iron ore remains constant in the model (\$45 t^{-1}, sensitivity tested between \$30 and 90 t^{-1}, (Finch Solutions, 2021)), although extrapolation of costs to lower grades is speculative given that these are not typically commercially sold. While carbonated slag may have a resale value, to be conservative, only the value derived from the sale of uncarbonated slag was subtracted from the annual expenditure. The cost of geological sequestration following capture was assumed to be a nominal \$10 tCO_2^{-1}(Schmelz et al., 2020). The net carbon emissions from the steelworks into the atmosphere was attributed a cost (e.g., simulating an emissions tax). If the operation resulted in a net removal of CO_2 from the atmosphere, this was accounted for as additional revenue (e.g., a traded credit on a CO_2 removals market) equivalent in magnitude but opposite in sign to the emissions cost.

The International Energy Agency (IEA) (IEA, 2012) estimate that approximately 1600 operating staff are required for a 4 Mt a^{-1} BF-BOF steelworks, which we assumed the same for the modelled steelworks given the same number of production steps. IEA (2012) suggest a workforce of 20 for a gas separation unit which we assume for the calcium looping system (although this may be conservative given that some of the labour cost may already been borne by those operating the base-case calciner). The operating workforce for the DRI, electrolyser and melting furnace was assumed to be the same as the BF-BOF (~600). We assume that the slag carbonation facility requires a workforce of approximately 100 people, as operating labour for slag management is already included in the BF-BOF estimates. We assumed \$120,000 a^{-1} as the operational labour cost (consistent with (IEA, 2012) but adjusted to 2019 with inflation).

2.12 Scaling and projections.

To explore the implications of the results to the global steel industry, projections of future steel production (based on a material economy saturation model see (Renforth, 2019)) were combined with background projections of energy costs, carbon prices, emissions intensity from CDR relevant integrated assessment model results (Strefler et al., 2021a) (Supplementary Figure 2) to drive the intervention scenarios. Projections for the base case were derived from the base-case SSP2 simulations in Luderer et al.,(2022) (Supplementary Tables 9-13. The model was simulated at annual intervals to generate projections of cost and emissions intensity of steel production linearly interpolated between IAM output years.

2.13 Uncertainty and sensitivity analysis.

A global sensitivity analysis was undertaken to assess input parametric uncertainty (Strunge et al., 2023). Normal probability density functions were applied to individual input parameters (although some were applied with uniform distributions, see Supplementary Tables 5, 6, and 8), and the model was sampled for 100 random selections in a Monte Carlo simulation at each time increment (e.g., 1 year) or ore-grade value (a total of 15,000 samples). A scatter plot analysis of the resulting model input-output is shown in Supplementary Figure 3. The range of outputs for both present and future static system backgrounds and timeseries

driven simulations was used to calculate 99% confidence intervals for the data, and the standard error associated with the key reported outcomes.

3.0 Results

3.1 Model validation.

Base case simulations for a BF-BOF steelworks (without implementing EAF for scrap recycling) using a common ore grade (65% Fe) feedstock suggests process requirements consistent with operating data from real steelworks (Figure 2), including total thermal energy (25 GJ t^{-1}), electrical energy (360 kWh t^{-1}), and CO_2 emissions (2.3 tCO_2 t^{-1}). By driving the model with data for energy (coal, natural gas, and electricity) and iron ore costs between 2010 and 2019, the simulated cost is reasonably consistent with historical prices for steel ($554-1116 t^{-1}), Figure 2G). Unsurprisingly, all simulated operational requirements increase with lower ore grades, although no publicly available plant data exists for low ore grades.

3.2 Comparison of intervention costs.

The model results suggest a levelised production cost of $476 t^{-1} for steel made using a conventional BF-BOF steelworks with EAF scrap recycling. Scenario A, which is intended to represent 'moderate' intervention, assumes that 25% of the iron ore is consumed in DRI (1:3 ratio between H_2 and CH_4 driven DRI), approximately 28% of the CO_2 in the process gas is captured using calcium looping and geologically stored, and 10% of the reductant in the blast furnace is produced from charcoal. This has a production cost of $516 t^{-1} of steel (26% increase to conventional BF-BOF steelworks). Scenario B is intended to represent a more ambitious intervention in which 50% of the ore is diverted to DRI, 95% of the CO_2 in the process emissions is captured and stored, and 20% of the reductant is replaced with charcoal. This has a cost of $716 t^{-1} of steel (68% increase to conventional BF-BOF steelworks). For comparison, we harmonised published technoeconomic assessments for a range of interventions (see Figure 3 and references therein), with the exception that our simulations consider additional processing (equivalent to reporting hot rolled coil), but the comparison data consider crude steel production. Our base case simulations were broadly consistent with that of a previously reported BF-BOF system(International Energy Agency, 2020). Adding monoethanolamine post-combustion capture to an existing BF-BOF steelworks carries estimated costs of $606 t^{-1} of steel. Replacing up to 52% of coal using biomass leads to estimated costs of $658 t^{-1} of steel or combining both strategies (i.e., replacing coal with biomass and adding post-combustion MEA capture) leads to estimated costs of $717 t^{-1} of steel). Similarly, our model results can be compared to costs estimated for emission reduction strategies for DRI-EAF steelworks which in itself could replace the BF-BOF route ($613 t^{-1} of steel), namely adding post-combustion capture to natural gas fuelled DRI processes ($660 t^{-1} of steel), or switching natural gas DRI processes to using hydrogen as a reduction agent (blue hydrogen: $737 t^{-1} of steel, green hydrogen $1215 t^{-1} of steel). This translates into an increase in costs of 7-110% (green hydrogen) while lowering the emissions by approximately 40 - 70%.

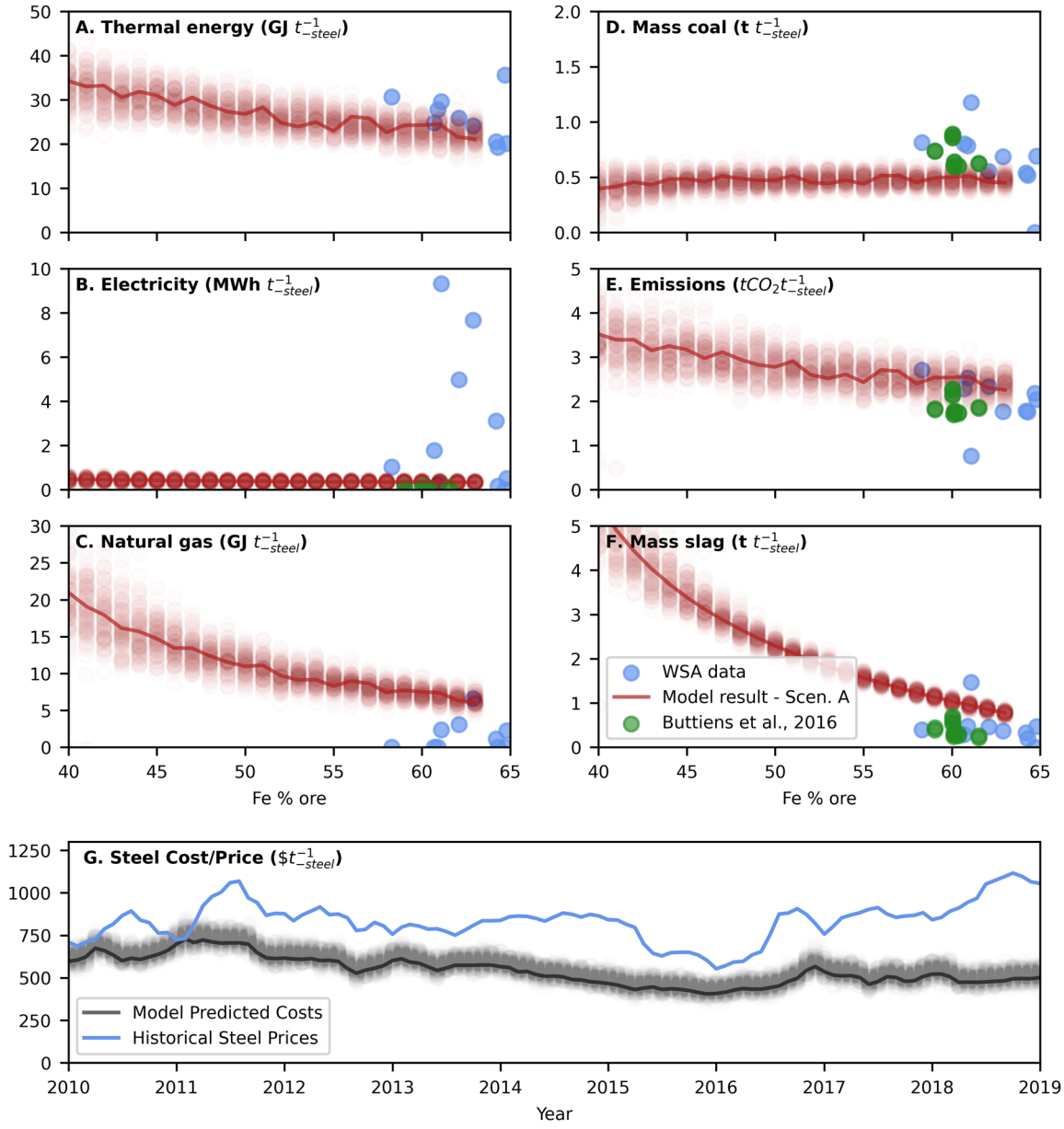

Figure 2. Model simulations showing the variation of A. thermal energy, B. electricity, C. natural gas, D. coal, E. CO_2 emissions, and F. slag production as a function of iron ore grade (from 40-65% Fe). Data from Buttiens et al.,(2016) and interpreted World Steel Data, supplied by the World Steel Association (personal communication 5th February 2020) are shown for comparison. G. The simulated cost of steel production from 2010 – 2019 in comparison to recorded steel prices over the same period.

Slag carbonation within the model was simulated by concentrating atmospheric CO_2 using a solid sorbent DAC (Young et al., 2023) and introducing it into a concrete basin containing water and slag. We assumed the most mature form of DAC is employed i.e., solid sorbent DAC using amine functionalised adsorbents in a temperature vacuum swing adsorption process. Costing and performance data for this process has been adapted from Young et al.(2023). This technology is designed to supply pure CO_2 for geological sequestration, which will also result in relatively faster reaction rates with slag. However, it may not be necessary to react slag with pure CO_2, which offers a possible avenue of optimisation between lower concentration DAC output and slag mineralisation.

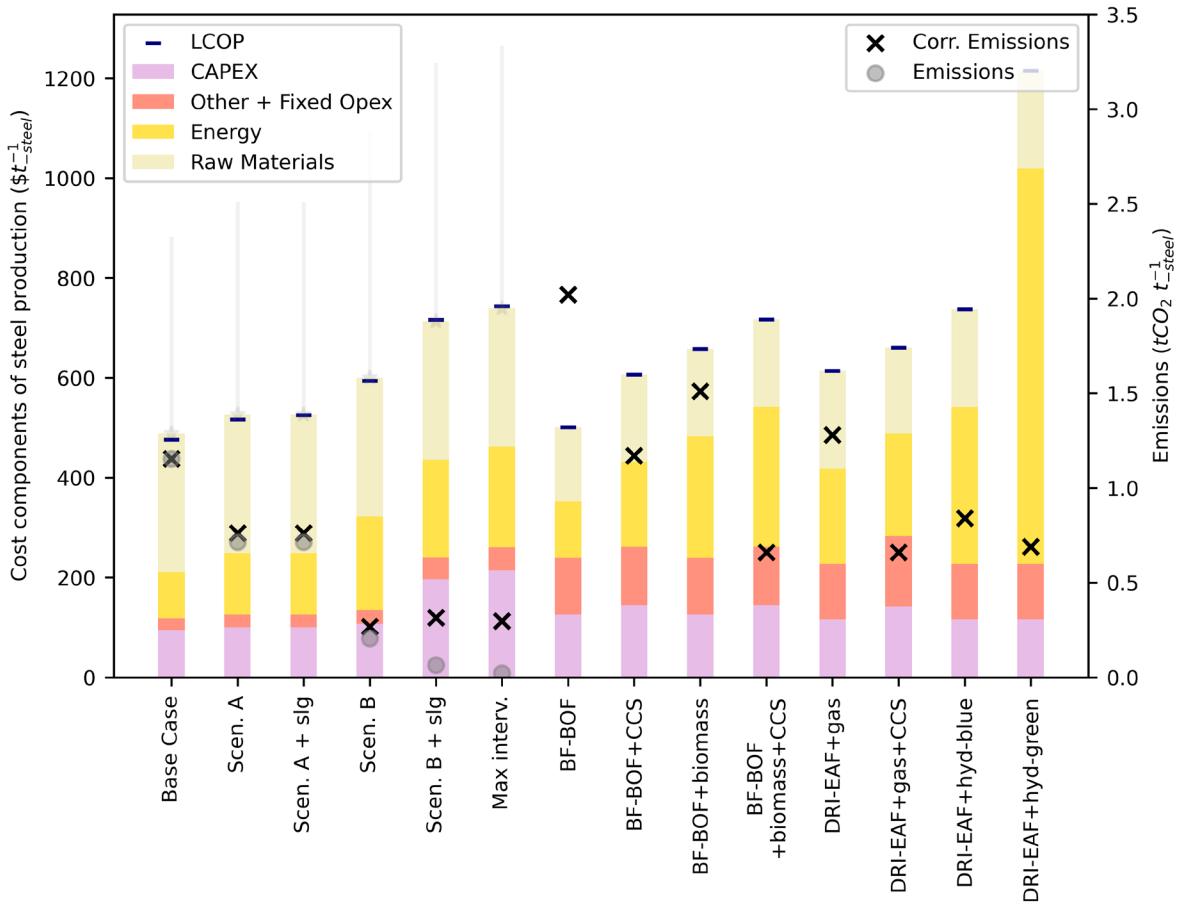

Figure 3. Comparison of the climate intervention approaches in the steel industry between the simulated model outcomes (using present day background system assumptions) and harmonized costs based on calculations from ("Frischknecht et al., 2007; IEA, 2012; International Energy Agency, 2020; Schuler et al., 2013) BF-BOF baseline assumptions from(Benavides et al., 2022; Damen et al., 2006; Fan and Friedmann, 2021) for BF-BOF interventions(IEA, 2012) and for DRI-EAF interventions (Fischedick et al., 2014) (the harmonisation procedure is described in Supplementary Text 2). Scenarios intended to represent a moderate (Scenario A) and ambitious (Scenario B) intervention, assumes that 25% and 50% of the iron ore is consumed in DRI, approximately 28% and 95% of the CO_2 in the process gas is captured using calcium looping and geologically stored, and 10% and 20% of the reductant in the blast furnace is produced from charcoal respectively. Intervention scenario emissions have been corrected to remove the impact of carbon dioxide removal (biomass CCS and slag carbonation) for comparison.

3.3 CO_2 emissions with ore grades.

Conventional methods of steel production result in 2.2 tCO_2 t^{-1} (Fan and Friedmann, 2021) consistent with our base-case scenario (2.3 tCO_2 t^{-1} without EAF scrap recycling, and 1.2 tCO_2 t^{-1} with scrap recycling, using present day background system assumptions). Moderate and ambitious application of climate intervention under 2050 background system assumptions (Scenario A and B), results in an emission intensity reduction to approximately 0.7 and 0.05 tCO_2 t^{-1} respectively. In both scenarios, the removal of CO_2 from the atmosphere and its reaction with slag further results in a lower CO_2 intensity of steel (0.3 and -0.1 tCO_2 t^{-1} respectively). With decreasing grades of ore, the CO_2 intensity of steel in scenarios A and B increased (Figure 4), but decreased with the introduction of slag

carbonation as more slag is produced per unit of steel. In all scenarios, the cost of steel increased with decreasing ore grades (assuming a value of \$200 tCO_2 for net CO_2 removal, and the inverse cost for CO_2 emission).

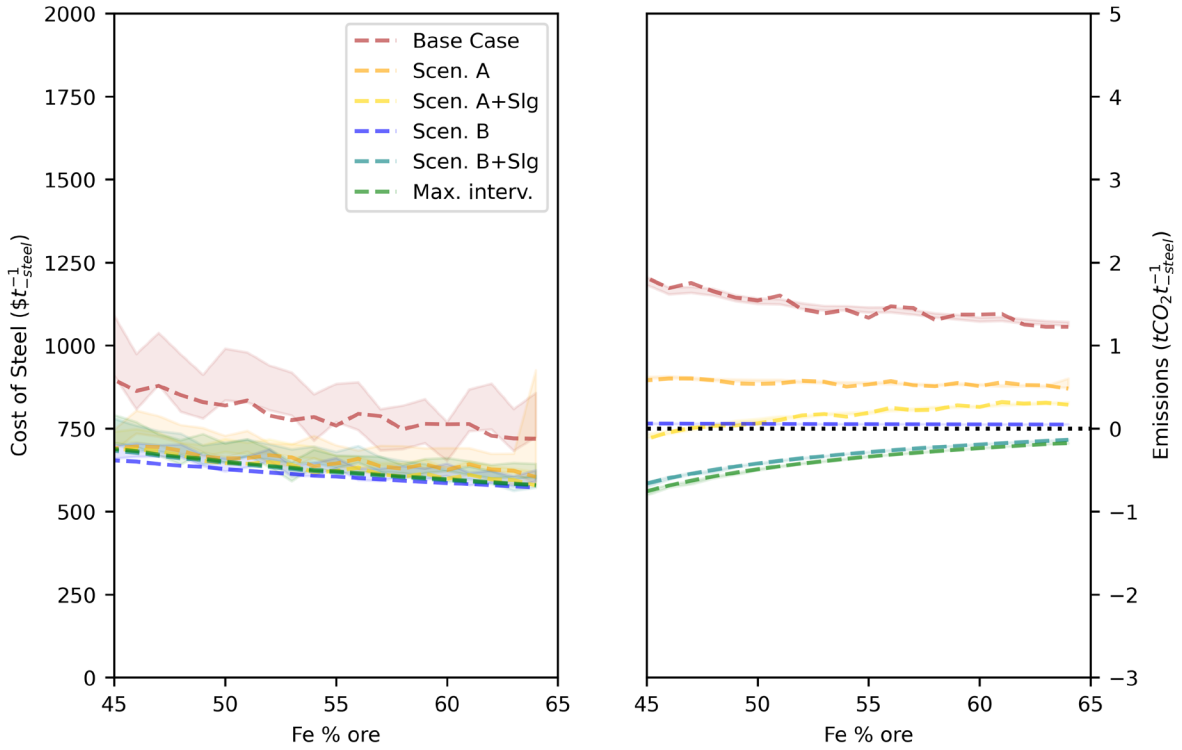

Figure 4. The cost (left) and emission intensity (right) of steel with varying grades of iron ore under a range of climate intervention scenarios and assumed CO_2 emissions cost/carbon dioxide removal credit of \$200 tCO_2^{-1}, and other background system drivers from 2050.

3.4 Steel costs under varying intervention incentives.

For simulations that use static background assumptions a cost of \$200 was attributed per net tonne of CO_2 released to the atmosphere, or -\$200 tCO_2^1 for a net removal of CO_2 from the atmosphere (e.g., in ambitious interventions that include charcoal use and slag carbonation). The model is agnostic regarding the governance of the incentivisation (e.g., carbon tax, cap and trade, government grants, voluntary or compulsory removal markets). Under this value the cost of steel production in the base-case BF-BOF unabated system may be \$719 t^{-1} of steel. Climate interventions in Scenarios A and B may be able to reduce the cost of steel \$604 and 572 t^{-1} respectively.

4.0 Discussion

While the emissions intensity of decarbonised steel could be further reduced and become deeply net negative with lower grade ores since more slag would be available, the model suggests that it would be uneconomical for steel producers to do this (Figure 5a). However, there may be a threshold in which a suitable incentivisation results in cost parity or cost reductions due to the use of lower grades of ore (Figure 5b and 5c).

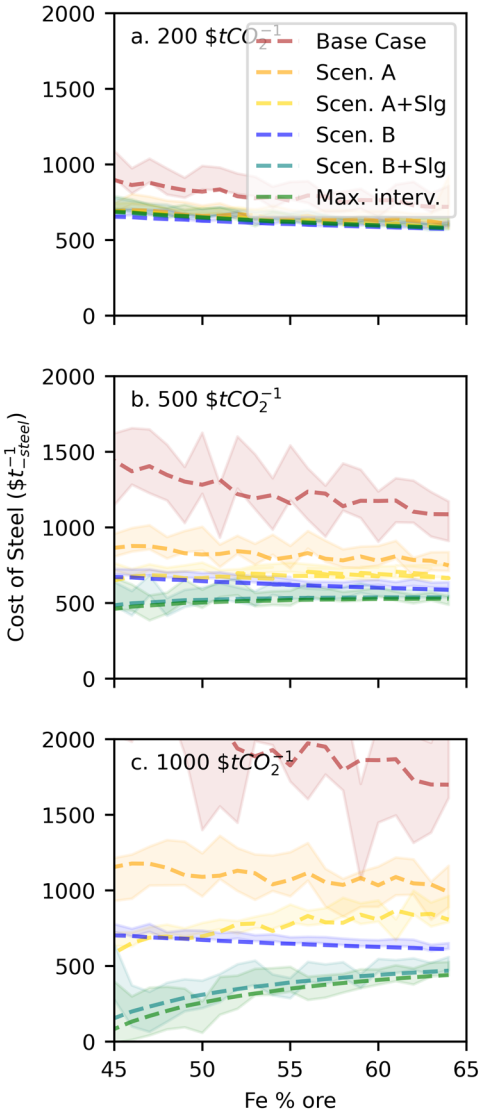

Figure 5. The cost of steel production against a range of iron ore grades under a range of emission reduction/CO_2 removal incentives (a-c).

Current incentives for emissions reduction are relatively low (e.g., ~\$100 tCO_2^{-1} recently in the European Emissions Trading Scheme). Integrated assessment models suggest cost of CO_2 may increase by \$100's to >\$1,000 by 2050 under a range of low emission pathways (Strefler et al., 2021b). Current voluntary removal purchasing schemes are apparently willing to pay multiple \$1,000's tCO_2^{-1}, although with a primary goal of instigating projects and stimulating research and development with the hope of future cost reductions (e.g., to between \$100- 600 tCO_2^{-1} (Young et al., 2023)). Harmonising incentivisation between emissions reduction and CO_2 removal will need to be done carefully, and may be facilitated by either separate regulation and/or incentivisation mechanisms (Young et al., 2023). However, some have suggested the combined approach of 'take-back obligations' (Jenkins et al., 2021).Therefore, it is plausible that the steel industry will be able to operate with an incentive for climate change intervention on the order of \$100's tCO_2^{-1}, and possibly greater. It is possible that the value of CO_2 reduction and removal will be sufficiently large to promote the use of lower grade ores, although the model suggests that this threshold is closer to \$500 than \$100 tCO_2^{-1}.

It is anticipated that steel production will continue to grow over the coming decades (Renforth, 2019), and if unabated, sector emissions would similarly increase (Figure 6a, left). Ambitious intervention methods together with wider economic decarbonisation and the reaction of atmospheric CO_2 with slag could result in a net-negative steel industry by 2050 (Figure 6a, left). Using lower grade iron ore, and the subsequent carbonation of the larger volume of slag, could result in deeper net negative emissions on the order of several Gt by mid-century (Figure 6b, left). Globally, there may be on the order of 8 Gt of legacy slag deposits with a 3-4 $GtCO_2$ cumulative removal potential (Renforth et al., 2011), their reprocessing and remediation would result in a reduction in the environmental liability associated with this material. Incentivising and adapting the steel industry for the routine carbonation of slag could result in exploiting these legacy deposits.

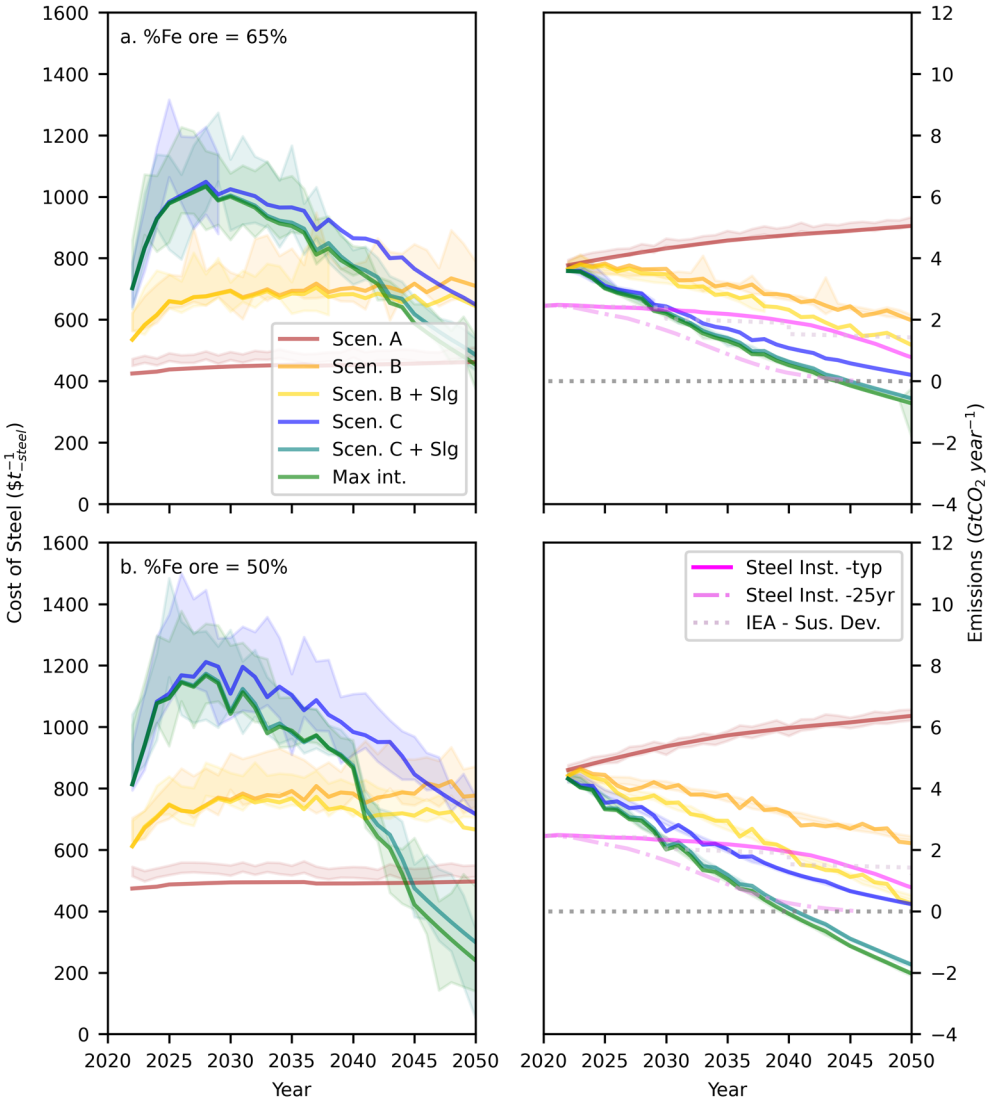

Figure 6. Costs of steel production (left) and global direct and indirect emissions from the steel industry (right) under a range of intervention scenarios. Top panels a) show projections based on a typically used ore grade (Fe = 65%) and the bottom panels project the use of a lower-grade ore (Fe = 50%). Steel production forecasts were based on the 'middle of the road' shared socio-economic pathway interpreted through a material saturation model(Renforth, 2019) and background system drivers were derived from integrated

assessment model results(Luderer et al., 2022; Strefler et al., 2021a). These emissions projections are broadly consistent with direct emission pathways included in the Steel Institute's PlantFact database (typical and 25-year investment timelines) and those in the sustainable development pathway from the IEA (see (International Energy Agency, 2020)and references therein).

The reduction in ore-grade is potentially limited by the presence of 'tramp' and alloying elements (e.g., Cu, Ni, Sn, As, Cr, Mo, Pb) which could be incorporated into the steel, and affect its mechanical behaviour. Using a concentration difference between an iron ore formation and its tailings repository, it is possible to estimate the impact of potentially problematic elements (Supplementary Table 1). Elements associated with the iron oxides within the ore (particularly Mn) will not be impacted by the changing ore grade, similarly others may be in relatively low concentration (Mo, Pb, Sb). Some elements may be sufficiently concentrated to prevent the use of low ore grades from some steel applications (Cr, Cu, Ni, V), and some may prevent the use of low ore grades in all steel applications (Co and Zn, to 52% and 44% Fe respectively). The limits presented in Supplementary Table 1, conservatively assume that all the elements are partitioned into the steel. However, a large proportion of Zn within a blast furnace evolves within the dust/off-gas (Ma, 2016), and many of the other elements are partitioned into phases within the slag (Proctor et al., 2000). Monitoring and selection of suitable lower-grade iron ore for specific steel applications and quantification of portioning into melt Fe would be required to maintain mechanical performance.

In addition to slag, alkaline materials are produced as by-products from the cement industry (cement kiln dust), aluminium refining (red mud), and mining (tailings). The ambient reaction of atmospheric CO_2 with other anthropogenically produced alkaline materials could be a relatively inexpensive method of CDR (Stolaroff et al., 2005), with potential to remove Gt of CO_2 per year from the atmosphere by 2050 (Renforth, 2019).

The most significant implication of this work is the potential of commercially exploiting lower-grade ores for steel manufacturing and CO_2 removal. The drive for high-grade ores has resulted in the expansion of ore production by countries with suitable deposits, the extensive beneficiation of ores, and the production of iron ore tailing facilities. Global reserves of iron ore contain on average ~50% Fe (Holmes et al., 2022), which even under moderate mitigation and incentivisation scenarios may be exploited directly for steel production and CO_2 removal. Lower grade ore deposits may include those from previously worked formations in developed countries (e.g., sintered Lias UK ironstone 38% Fe (Goldring and Juckes, 2001), or Precambrian banded iron formation around Lake Superior US in which half the deposit is <50% Fe (Cox and Singer, 1986)), iron ore tailing facilities (27% Fe, (Carneiro et al., 2023)), saprolite laterites (16% Fe (Tian et al., 2020)), and some legacy slag deposits (10-30% Fe,(Riley et al., 2020))

Conclusions

Steel is essential for economic development, and production/technology pathways resulting in low greenhouse gas emissions are required for the industry to contribute to climate change targets. Here we developed a model that simulates the technoeconomics of steel production (including energy and raw material requirements, CO_2 emissions, and levelized cost of production) for a base-case blast furnace/basic oxygen furnace system. The results of which appear to be consistent with present and historical data for a range of model indicator values. We use both static and prospective technoeconomic modelling to simulate

the cost and CO_2 emissions of steel production for progressively ambitious climate interventions in foreground technologies (directly reduced iron, scrap recycling using an electrical arc furnace, carbon capture and storage) in which the background system is driven by the results of an integrative assessment model. We also simulate CO_2 removal pathways in the steel industry through the use of biomass based reductants and atmospheric CO_2 reaction with by-product slag.

The model results suggest that unabated emissions (penalised at \$200 tCO_2^{-1}) would result in the cost of steel production increasing to >\$700 t^{-1}. Deep emission reduction scenarios coupled with CO_2 removal could result in total costs of steel on the order of ~\$600 t^{-1}. The most ambitious intervention scenario results in net negative CO_2 steel, in which the additional costs of mitigation are wholly compensated for by the value of CO_2 removal. The most important, and unexpected implication of this work is that incentivising CO_2 removal (~\$100's tCO_2^{-1}) in a low-emission steel industry, could result in economic exploitation of lower-grade iron ore and possibly alleviating some of the predicted pressures of decreasing global ore grades.

Acknowledgements

The authors acknowledge funding from the Industrial Decarbonisation Research Centre (EP/V027050/1), and from UKRI greenhouse gas removal research programme (NE/P019943/1). The authors would like to thank Andrew Purvis of the World Steel Association for supplying data used in Figure 2. Dr Lukas Küng is thanked for his helpful comments during the development of this work.

Author Contributions

PR – Conceptualisation, funding acquisition, primary model development and simulation, drafting, editing.

JC, SF, EC – Slag carbonation model development, model input data, drafting, editing

JY – Direct air capture model development, model input data, drafting, editing

TS – Climate change interventions model input data, drafting, editing

AR – Slag after use model input data, drafting, editing

WM -Funding acquisition, drafting, editing

MvS - Funding acquisition, drafting, editing

References

Allen, M.R., Frame, D.J., Huntingford, C., Jones, C.D., Lowe, J.A., Meinshausen, M., Meinshausen, N., 2009. Warming caused by cumulative carbon emissions towards the trillionth tonne. Nature 458, 1163–1166. https://doi.org/10.1038/nature08019

Benavides, K., Gurgel, A., Morris, J., Mignone, B., Chapman, B., Kheshgi, H., Herzog, H., Paltsev, S., 2022. Emission Mitigation in the Global Steel Industry: Representing CCS and Hydrogen Options in Integrated Assessment Modeling. SSRN Electronic Journal. https://doi.org/10.2139/ssrn.4271699

Bhattacharya, A., Muthusamy, S., 2017. Static heat energy balance mathematical model for an iron blast furnace. International Journal of Mineral Processing and Extractive Metallurgy 2, 57–67. https://doi.org/10.11648/j.ijmpem.20170205.11

Bonenfant, D., Kharoune, L., Sauvé, S., Hausler, R., Niquette, P., Mimeault, M., Kharoune, M., 2008. CO_2 Sequestration by Aqueous Red Mud Carbonation at Ambient Pressure and Temperature. Ind. Eng. Chem. Res. 47, 7617–7622. https://doi.org/10.1021/ie7017228

Buttiens, K., Leroy, J., Negro, P., Thomas, J.-S., Edwards, K., De Lassat, Y., 2016. The Carbon Cost of Slag Production in the Blast Furnace: A Scientific Approach. Journal of Sustainable Metallurgy 2, 62–72. https://doi.org/10.1007/s40831-016-0046-8

Carneiro, J.J.V., Marques, E.A.G., Viana da Fonseca, A.J.P., Ferraz, R.L., Oliveira, Â.H.C., 2023. Characterization of an Iron Ore Tailing Sample and the Evaluation of Its Representativeness. Geotechnical and Geological Engineering 41, 2833–2852. https://doi.org/10.1007/s10706-023-02430-8

Clout, J.M.F., Manuel, J.R., 2015. 2 - Mineralogical, chemical, and physical characteristics of iron ore, in: Lu, L. (Ed.), Iron Ore. Woodhead Publishing, pp. 45–84. https://doi.org/10.1016/B978-1-78242-156-6.00002-2

Committee on Developing a Research Agenda for Carbon Dioxide Removal and Reliable Sequestration, Board on Atmospheric Sciences and Climate, Board on Energy and Environmental Systems, Board on Agriculture and Natural Resources, Board on Earth Sciences and Resources, Board on Chemical Sciences and Technology, Ocean Studies Board, Division on Earth and Life Studies, National Academies of Sciences, Engineering, and Medicine, 2019. Negative Emissions Technologies and Reliable Sequestration: A Research Agenda. National Academies Press, Washington, D.C. https://doi.org/10.17226/25259

Cox, D.P., Singer, D.A., 1986. Mineral deposit models. USGPO,.

Damen, K., Troost, M. van, Faaij, A., Turkenburg, W., 2006. A comparison of electricity and hydrogen production systems with CO2 capture and storage. Part A: Review and selection of promising conversion and capture technologies. Progress in Energy and Combustion Science 32, 215–246. https://doi.org/10.1016/j.pecs.2005.11.005

Deutz, P., Baxter, H., Gibbs, D., Mayes, W.M., Gomes, H.I., 2017. Resource recovery and remediation of highly alkaline residues: A political-industrial ecology approach to building a circular economy. Geoforum 85, 336–344. https://doi.org/10.1016/j.geoforum.2017.03.021

Dubey, M.K., Ziock, H., Rueff, G., Smith, W.S., Colman, J., Elliott, S., Lackner, K., Johnston, N.A., 2002. Carbon Dioxide Extraction from the Atmosphere Through Engineered Chemical Sinkage: Enabling Energy and Environmental Security, in: AGU Spring Meeting Abstracts. pp. GC31A-03.

EPA, 1995. Protocol for equipment leak emissions estimates (No. EPA-453/R-95-017). United States Environmental Protection Agency.

Facchini, F., Mossa, G., Mummolo, G., Vitti, M., 2021. An Economic Model to Assess Profitable Scenarios of EAF-Based Steelmaking Plants under Uncertain Conditions. Energies 14. https://doi.org/10.3390/en14217395

Fan, Z., Friedmann, S.J., 2021. Low-carbon production of iron and steel: Technology options, economic assessment, and policy. Joule 5, 829–862. https://doi.org/10.1016/j.joule.2021.02.018

Finch Solutions, 2021. Global Iron Ore Mining Outlook. Fitch Solutions Group Ltd.

Fischedick, M., Marzinkowski, J., Winzer, P., Weigel, M., 2014. Techno-economic evaluation of innovative steel production technologies. Journal of Cleaner Production 84, 563–580. https://doi.org/10.1016/j.jclepro.2014.05.063

Friedrich, B., Kalisch, M., Friedmann, D., Degel, R., Kaußen, F., Böhlke, J., 2018. The Submerged Arc Furnace (SAF): State-of-the-Art Metal Recovery from Nonferrous Slags. Journal of Sustainable Metallurgy 4, 77–94. https://doi.org/10.1007/s40831-017-0153-1

"Frischknecht, R. [Ecoinvent C., Swiss Federal Laboratories for Materials Testing and Research (EMPA), Duebendorf (Switzerland)]", "Jungbluth, N. [ESU-services L., Uster (Switzerland)]", "Althaus, H.-J., "Hischier, R. [Swiss F.L. for M.T. and R. (EMPA), Duebendorf (Switzerland)]", "Doka, G. [Doka L.C.A. (LCA), Zuerich (Switzerland)]", "Dones, R., "Heck, T. [Paul S.I. (PSI), Villigen (Switzerland)]", "Hellweg, S., "Wernet, G. [Swiss F.I. of T. (ETHZ), Institute for Chemicals and Bioengineering (ICB), Zuerich (Switzerland)]", "Nemecek, T. [Forschungsanstalt A.R.-T. (ART), Zuerich (Switzerland)]", "Rebitzer, G. [Swiss F.I. of T. (EPFL), Lausanne (Switzerland)]", "Spielmann, M. [Swiss F.I. of T. (ETHZ), Institute for Environmental Decisions, Natural and Social Science Interface (UNS), Zuerich (Switzerland)]", 2007. Overview and methodology. Data v2.0 (2007). Ecoinvent report No. 1, []. Switzerland.

Gan, Y., Griffin, W.M., 2018. Analysis of life-cycle GHG emissions for iron ore mining and processing in China—Uncertainty and trends. Resources Policy 58, 90–96. https://doi.org/10.1016/j.resourpol.2018.03.015

Goldring, D.C., Juckes, L.M., 2001. Iron ore supplies to the United Kingdom iron and steel industry. Mining Technology 110, 75–85. https://doi.org/10.1179/mnt.2001.110.2.75

Guo, J., Bao, Y., Wang, M., 2018. Steel slag in China: Treatment, recycling, and management. Waste Management 78, 318–330. https://doi.org/10.1016/j.wasman.2018.04.045

Hobson, A.J., Stewart, D.I., Bray, A.W., Mortimer, R.J.G., Mayes, W.M., Riley, A.L., Rogerson, M., Burke, I.T., 2018. Behaviour and fate of vanadium during the aerobic neutralisation of hyperalkaline slag leachate. Science of The Total Environment 643, 1191–1199. https://doi.org/10.1016/j.scitotenv.2018.06.272

Holmes, R.J., Lu, Y., Lu, L., 2022. Chapter 1 - Introduction: Overview of the global iron ore industry, in: Lu, L. (Ed.), Iron Ore (Second Edition). Woodhead Publishing, pp. 1–56. https://doi.org/10.1016/B978-0-12-820226-5.00023-9

Hooey, L., Tobiesen, A., Johns, J., Santos, S., 2013. Techno-economic Study of an Integrated Steelworks Equipped with Oxygen Blast Furnace and CO2 Capture. Energy Procedia 37, 7139–7151. https://doi.org/10.1016/j.egypro.2013.06.651

Huijgen, W.J.J., Comans, R.N.J., 2006. Carbonation of Steel Slag for CO_2 Sequestration: Leaching of Products and Reaction Mechanisms. Environ. Sci. Technol. 40, 2790–2796. https://doi.org/10.1021/es052534b

Huijgen, W.J.J., Comans, R.N.J., Witkamp, G.-J., 2007. Cost evaluation of CO2 sequestration by aqueous mineral carbonation. Energy Conversion and Management 48, 1923–1935. https://doi.org/10.1016/j.enconman.2007.01.035

Huijgen, W.J.J., Witkamp, G.-J., Comans, R.N.J., 2005. Mineral CO_2 Sequestration by Steel Slag Carbonation. Environ. Sci. Technol. 39, 9676–9682. https://doi.org/10.1021/es050795f

IEA, 2012. Understanding the Economics of Deploying CO2 Capture Technologies in an Integrated Steel Mill. International Energy Agency.

International Energy Agency, 2020. Iron and Steel Technology Roadmap: Towards More Sustainable Steelmaking. OECD Publishing.

Jenkins, S., Mitchell-Larson, E., Ives, M.C., Haszeldine, S., Allen, M., 2021. Upstream decarbonization through a carbon takeback obligation: An affordable backstop climate policy. Joule 5, 2777–2796. https://doi.org/10.1016/j.joule.2021.10.012

Jesus, M., Napoli, A., Trugilho, P., Junior, A., Mendoza Martinez, C., Freitas, T., 2018. Energy and mass balance in the pyrolysis process of eucalyptus wood. CERNE 24, 288–294. https://doi.org/10.1590/01047760201824032561

Kobelev, V.A., Puzanov, V.P., Nechkin, G.A., 2015. Melting temperatures of iron-ore sinter. Steel in Translation 45, 856–862. https://doi.org/10.3103/S0967091215110121

Küng, L., Aeschlimann, S., Charalambous, C., McIlwaine, F., Young, J., Shannon, N., Strassel, K., Maesano, C.N., Kahsar, R., Pike, D., Garcia, S., 2023. A Roadmap for Achieving Scalable, Safe, and Low-cost Direct Air Carbon Capture and Storage.

Luderer, G., Madeddu, S., Merfort, L., Ueckerdt, F., Pehl, M., Pietzcker, R., Rottoli, M., Schreyer, F., Bauer, N., Baumstark, L., Bertram, C., Dirnaichner, A., Humpenöder, F., Levesque, A., Popp, A., Rodrigues, R., Strefler, J., Kriegler, E., 2022. Impact of declining renewable energy costs on electrification in low-emission scenarios. Nature Energy 7, 32–42. https://doi.org/10.1038/s41560-021-00937-z

Ma, N., 2016. Recycling of basic oxygen furnace steelmaking dust by in-process separation of zinc from the dust. Journal of Cleaner Production 112, 4497–4504. https://doi.org/10.1016/j.jclepro.2015.07.009

Madhavan, N., Brooks, G.A., Rhamdhani, M.A., Rout, B.K., Schrama, F.N.H., Overbosch, A., 2021. General mass balance for oxygen steelmaking. Ironmaking & Steelmaking 48, 40–54. https://doi.org/10.1080/03019233.2020.1731252

Mandova, H., Leduc, S., Wang, C., Wetterlund, E., Patrizio, P., Gale, W., Kraxner, F., 2018. Possibilities for CO2 emission reduction using biomass in European integrated steel plants. Biomass and Bioenergy 115, 231–243. https://doi.org/10.1016/j.biombioe.2018.04.021

Masson-Delmotte, V., Zhai, P., Pörtner, H.-O., Roberts, D., Skea, J., Shukla, P.R., 2022. Global Warming of 1.5° C: IPCC Special Report on Impacts of Global Warming of 1.5° C above Pre-industrial Levels in Context of Strengthening Response to Climate Change, Sustainable Development, and Efforts to Eradicate Poverty. Cambridge University Press.

Mayes, W.M., Riley, A.L., Gomes, H.I., Brabham, P., Hamlyn, J., Pullin, H., Renforth, P., 2018. Atmospheric CO_2 Sequestration in Iron and Steel Slag: Consett, County Durham, United Kingdom. Environ. Sci. Technol. 52, 7892–7900. https://doi.org/10.1021/acs.est.8b01883

Mousa, E., Wang, C., Riesbeck, J., Larsson, M., 2016. Biomass applications in iron and steel industry: An overview of challenges and opportunities. Renewable and Sustainable Energy Reviews 65, 1247–1266. https://doi.org/10.1016/j.rser.2016.07.061

Myers, C., Nakagaki, T., 2020. Direct mineralization of atmospheric CO2 using natural rocks in Japan. Environmental Research Letters 15, 124018. https://doi.org/10.1088/1748-9326/abc217

Nunes, V.A., Borges, P.H.R., 2021. Recent advances in the reuse of steel slags and future perspectives as binder and aggregate for alkali-activated materials. Construction and Building Materials 281, 122605. https://doi.org/10.1016/j.conbuildmat.2021.122605

Otto, A., Robinius, M., Grube, T., Schiebahn, S., Praktiknjo, A., Stolten, D., 2017. Power-to-Steel: Reducing CO2 through the Integration of Renewable Energy and Hydrogen into the German Steel Industry. Energies 10. https://doi.org/10.3390/en10040451

Paris Agreement, 2015. Paris Agreement. Presented at the Report of the Conference of the Parties to the United Nations Framework Convention on Climate Change (21st Session, 2015: Paris). Retrived December, HeinOnline, p. 2017.

Peacey, J.G., Davenport, W.G., 2016. The iron blast furnace: theory and practice. Elsevier.

Proctor, D.M., Fehling, K.A., Shay, E.C., Wittenborn, J.L., Green, J.J., Avent, C., Bigham, R.D., Connolly, M., Lee, B., Shepker, T.O., Zak, M.A., 2000. Physical and Chemical Characteristics of Blast Furnace, Basic Oxygen Furnace, and Electric Arc Furnace Steel Industry Slags. Environ. Sci. Technol. 34, 1576–1582. https://doi.org/10.1021/es9906002

Pullin, H., Bray, A.W., Burke, I.T., Muir, D.D., Sapsford, D.J., Mayes, W.M., Renforth, P., 2019. Atmospheric Carbon Capture Performance of Legacy Iron and Steel Waste. Environ. Sci. Technol. 53, 9502–9511. https://doi.org/10.1021/acs.est.9b01265

Rasul, M.G., Tanty, B.S., Mohanty, B., 2007. Modelling and analysis of blast furnace performance for efficient utilization of energy. Applied Thermal Engineering 27, 78–88. https://doi.org/10.1016/j.applthermaleng.2006.04.026

Ren, M., Lu, P., Liu, X., Hossain, M.S., Fang, Y., Hanaoka, T., O'Gallachoir, B., Glynn, J., Dai, H., 2021. Decarbonizing China's iron and steel industry from the supply and demand sides for carbon neutrality. Applied Energy 298, 117209. https://doi.org/10.1016/j.apenergy.2021.117209

Renforth, P., 2019. The negative emission potential of alkaline materials. Nat Commun 10, 1401. https://doi.org/10.1038/s41467-019-09475-5

Renforth, P., Manning, D.A.C., Lopez-Capel, E., 2009. Carbonate precipitation in artificial soils as a sink for atmospheric carbon dioxide. Applied Geochemistry 24, 1757–1764. https://doi.org/10.1016/j.apgeochem.2009.05.005

Renforth, P., Washbourne, C.-L., Taylder, J., Manning, D.A.C., 2011. Silicate Production and Availability for Mineral Carbonation. Environ. Sci. Technol. 45, 2035–2041. https://doi.org/10.1021/es103241w

Riley, A., Cameron, J., Burke, I., Onnis, P., MacDonald, J., Gandy, C., Crane, R., Byrne, P., Comber, S., Jarvis, A., Edwards, karen, Mayes, W., 2023. Environmental Behaviour of Iron and Steel Slags in Coastal Settings. https://doi.org/10.2139/ssrn.4446615

Riley, A.L., MacDonald, J.M., Burke, I.T., Renforth, P., Jarvis, A.P., Hudson-Edwards, K.A., McKie, J., Mayes, W.M., 2020. Legacy iron and steel wastes in the UK: Extent, resource potential, and management futures. Journal of Geochemical Exploration 219, 106630. https://doi.org/10.1016/j.gexplo.2020.106630

Salman, Chaudhary Awais, 2014. Techno-economic analysis of wood pyrolysis in Sweden. https://doi.org/10.13140/RG.2.2.11367.19369

Schmelz, W.J., Hochman, G., Miller, K.G., 2020. Total cost of carbon capture and storage implemented at a regional scale: northeastern and midwestern United States. Interface Focus 10, 20190065. https://doi.org/10.1098/rsfs.2019.0065

Schuler, F., Voigt, N., Schmidt, T., Woertler, M., Dahlmann, P., Ghenda, J.-T., Luengen, H., 2013. Steel's Contribution to a Low-Carbon Europe 2050. Stahl und Eisen 133, 61–63.

Steelonthenet, 2023. Electric Arc Furnace Steelmaking Costs 2023: Conversion costs for electric arc steelmaking.

Stolaroff, J.K., Lowry, G.V., Keith, D.W., 2005. Using CaO- and MgO-rich industrial waste streams for carbon sequestration. Energy Conversion and Management 46, 687–699. https://doi.org/10.1016/j.enconman.2004.05.009

Strefler, J., Bauer, N., Humpenöder, F., Klein, D., Popp, A., Kriegler, E., 2021a. Carbon dioxide removal technologies are not born equal. Environmental Research Letters 16, 074021. https://doi.org/10.1088/1748-9326/ac0a11

Strefler, J., Kriegler, E., Bauer, N., Luderer, G., Pietzcker, R.C., Giannousakis, A., Edenhofer, O., 2021b. Alternative carbon price trajectories can avoid excessive carbon removal. Nature Communications 12, 2264. https://doi.org/10.1038/s41467-021-22211-2

Strunge, T., Renforth, P., Van der Spek, M., 2023. Uncertainty quantification in the techno-economic analysis of emission reduction technologies: a tutorial case study on CO2 mineralization. Frontiers in Energy Research 11. https://doi.org/10.3389/fenrg.2023.1182969

Strunk, P., 2020. Slag recycling. Recovery: Recycling Technology Worldwide.

Tanzer, S.E., Blok, K., Ramírez, A., 2020. Can bioenergy with carbon capture and storage result in carbon negative steel? International Journal of Greenhouse Gas Control 100, 103104. https://doi.org/10.1016/j.ijggc.2020.103104

Tian, H., Pan, J., Zhu, D., Yang, C., Guo, Z., Xue, Y., 2020. Improved beneficiation of nickel and iron from a low-grade saprolite laterite by addition of limonitic laterite ore and CaCO3. Journal of Materials Research and Technology 9, 2578–2589. https://doi.org/10.1016/j.jmrt.2019.12.088

Tian, S., Jiang, J., Zhang, Z., Manovic, V., 2018. Inherent potential of steelmaking to contribute to decarbonisation targets via industrial carbon capture and storage. Nature Communications 9, 4422. https://doi.org/10.1038/s41467-018-06886-8

van der Spek, M., Fout, T., Garcia, M., Kuncheekanna, V.N., Matuszewski, M., McCoy, S., Morgan, J., Nazir, S.M., Ramirez, A., Roussanaly, S., Rubin, E.S., 2020. Uncertainty analysis in the techno-economic assessment of CO2 capture and storage technologies. Critical review and guidelines for use. International Journal of Greenhouse Gas Control 100, 103113. https://doi.org/10.1016/j.ijggc.2020.103113

Vogl, V., Åhman, M., Nilsson, L.J., 2018. Assessment of hydrogen direct reduction for fossil-free steelmaking. Journal of Cleaner Production 203, 736–745. https://doi.org/10.1016/j.jclepro.2018.08.279

Wang, P., Ryberg, M., Yang, Y., Feng, K., Kara, S., Hauschild, M., Chen, W.-Q., 2021. Efficiency stagnation in global steel production urges joint supply- and demand-side mitigation efforts. Nature Communications 12, 2066. https://doi.org/10.1038/s41467-021-22245-6

Wendling, L.A., Binet, M.T., Yuan, Z., Gissi, F., Koppel, D.J., Adams, M.S., 2013. Geochemical and ecotoxicological assessment of iron- and steel-making slags for potential use in environmental applications. Environmental Toxicology and Chemistry 32, 2602–2610. https://doi.org/10.1002/etc.2342

Woods, D.R., 2007. Rules of thumb in engineering practice. Wiley-VCH, Weinheim.

World Steel Association, 2023. 2023 World Steel in Figures. World Steel Association, Brussels, Belgium.

Wörtler, M., Schuler, F., Voigt, N., Schmidt, T., Dahlmann, P., Lüngen, H.B., Ghenda, J.-T., 2013. Steel's contribution to a low-carbon Europe 2050: Technical and economic analysis of the sector's CO2 abatement potential. London: BCG. Retrieved April 20, 2015.

Young, J., McQueen, N., Charalambous, C., Foteinis, S., Hawrot, O., Ojeda, M., Pilorgé, H., Andresen, J., Psarras, P., Renforth, P., 2023. The cost of direct air capture and storage can be reduced via strategic deployment but is unlikely to fall below stated cost targets. One Earth 6, 899–917. https://doi.org/10.1016/j.oneear.2023.06.004

Zhang, Y., Li, Z., Aviso, K.B., Tan, R.R., Wang, F., Jia, X., 2023. Multi-period optimization for CO2 sequestration potential of enhanced weathering using non-hazardous industrial wastes. Resources, Conservation and Recycling 189, 106766. https://doi.org/10.1016/j.resconrec.2022.106766